PHYTRA4 – The Fourth International Conference on Physics and Technology of Reactors and Applications.
Marrakech, Morocco, September 17-19, 2018, on CD-ROM, GMTR, Rabat, Morocco (2018)

COMBINING THE TONE'S AND SUBGROUP MODELS FOR REFERENCE LWR SELF-SHIELDING CALCULATIONS IN APOLLO3®

J-F. Vidal, Damien Raynaud

CEA, DEN, DER/SPRC Cadarache, F-13108 Saint Paul-Lez-Durance, France.

jean-francois.vidal@cea.fr

ABSTRACT

The new deterministic platform APOLLO3® offers three different self-shielding models:

- the Sanchez-Coste model currently used in APOLLO2 for Light Water Reactors production calculations,
- the subgroup method of ECCO used for Fast Reactors applications,
- the recently implemented Tone method specifically dedicated to Fast Reactors calculations.

The Sanchez-Coste method is based on an equivalence in dilution and lies on some hypothesis (pure elastic scattering, fine structure factorization) that are not always relevant, especially in case of voiding or for large metallic bulk treatment. Following a previous work based on the APOLLO2 subgroup method, this paper confirms more deeply the accuracy of the ECCO subgroup method in all kind of situations and establishes it as a reference self-shielding method for Light Water Reactor calculations with APOLLO3®. Using a 383-group energy mesh, it is shown that the Tone method can be substituted at the subgroup method at high energy (E > 3 keV) without loss of precision, allowing a significant reduction of the calculation time. It can be used alone for less demanding design studies, provided a uniform temperature distribution in fuel.

Key Words: Light Water Reactor, Resonance self-shielding methods, Subgroup, Tone, APOLLO3® code

1. INTRODUCTION

The new deterministic platform APOLLO3® [1] offers three different self-shielding methods:

- the Sanchez-Coste method currently used in APOLLO2 [2] for Light Water Reactors (LWR) production calculations,
- the subgroup method of ECCO [3] used for Fast Reactors applications [4, 5],
- the recently implemented Tone's method [6] specifically dedicated to Fast Reactors calculations [7].

The Sanchez-Coste method is an extension to several resonant isotopes in several regions of the Livolant-Jeanpierre formalism implemented in the APOLLO1 code [8]. It is based on an heterogeneous-homogeneous equivalence and lies on some hypothesis (pure elastic scattering, fine

structure factorization) that are well suited for Light Water Reactors in nominal situation but less relevant when dealing with fuel in voided configurations [9] or with large metallic bulk [10].

The Sanchez-Coste model is currently used with the 281-group SHEM energy mesh designed to avoid any self-shielding below 22.5 eV [13]. However, this mesh had been refined between 22.5 eV and 3 keV by Hébert and Santamarina (SHEM 361-group energy mesh [14]) to give satisfactory results for LWR calculations when using the subgroup method. Here, we are using a JEFF3.1.1 383-group library (REL383) whose energy mesh is derived from SHEM361 one[1].

The Tone's method was developed by Tatsuzo Tone in the mid-seventies for heterogeneous fast-spectrum analyses with fine or ultrafine energy group calculations [6] and was originally based on a heterogeneous-homogeneous equivalence. Recently, a new approach for this technique was implemented in APOLLO3® by Lei Mao [7] using the same probability tables than the subgroup method to integrate energy-dependent quantities. Very good results are obtained for Fast Reactor applications so that Tone's method is now commonly used at CEA in this case instead of the subgroup method.

Following this work, Hébert investigated, with the DRAGON5 lattice code, the accuracy of the Tone's method for PWR applications with a focus on distributed self-shielding effects [15, 16]. Performing slowing-down calculations with a purely elastic scattering kernel, he found in [16] that "the Tone's method is leading acceptable results with the SHEM295 energy mesh, with the exception of a 20% discrepancy (13% with the SHEM361 energy mesh) that is observed in the 5% volume external fuel ring". We consider on the contrary that the 1.4-1.6 % discrepancy observed on the ^{238}U integrated absorption rate in the whole UOX pellet (cf. Table 5 of [16]) is not acceptable regarding the target accuracy currently required for LWR reactors calculations[2]. In the same paper, we can observe that the subgroup method leads to discrepancies around 0.5 %, which is precisely the order of magnitude of the targeted accuracy.

Thus, the aim of the present work was to verify that the specific implementation of the Tone's method in APOLLO3 is giving the same trends than DRAGON5 for LWR applications and, beyond, to determine the energy below which this method is not precise enough. The idea is to use the Tone's method above this energy, the subgroup method, more accurate but also more expensive, being used below. This new self-shielding strategy (Tone + subgroup) is intended to replace the Sanchez-Coste method in APOLLO3® reference calculation schemes; both methods are therefore compared here.

To make sure there is no compensation between the different isotopes and reaction rates, we perform a microscopic validation of APOLLO3® results (using the Sanchez-Coste, the subgroup and the Tone's self-shielding methods) against continuous energy Monte Carlo TRIPOLI-4® [17] ones in critical mode (to include the fission and inelastic scattering sources issues). Thereby, an absorption (capture + fission) rate comparison is done isotope by isotope for the 281-group SHEM281 and 383-group REL383 energy meshes and for a more synthetic 13-group one (defined

[1] A few groups delivered by Hébert in the 315-group Dragon library [20] have been added between 1 and 10 keV around the 2.85 keV neutron resonance of sodium to allow its use for Fast Reactors calculations but they are not necessary for LWR ones.

[2] In our UOX cell critical calculation, ^{238}U absorption rate value represents about 27000 pcm of the total absorption, so a 1.5% relative discrepancy on this absorption rate corresponds roughly to a 500-pcm discrepancy on the infinite multiplication factor (assuming a 1.3 value for k_{inf}).

in [9] and reminded Table I). The aim is to identify precisely which absorbing resonances have discrepancies for each method and status the energy limit for the use of the Tone's method.

Table I. 13-group energy mesh for self-shielding validation.

Group	Upper Boundary	Lower Boundary	Comments
1	19.74 MeV	2.24 MeV	(n,xn) threshold U238 (6.2 MeV) and O16 inelastic threshold (6.4 MeV). 2nd and 3rd chance fissions
2	2.24 MeV	498 keV	Fission threshold U238 (approx. 1 MeV), 2nd and 3rd resonance of O16 (1 MeV and 1.31 MeV resp.)
3	498 keV	11.14 keV	1st resonance of O16 (434 keV), unresolved domain for heavy isotopes, inelastic threshold for U238 (45 keV)
4	11.14 keV	752 eV	Resolved-unresolved limit for U238
5	752 eV	76.2 eV	Resonance of Zr91 (291 eV), beginning of resolved domain, resonances of U238 (102 eV, 117 eV, 189 eV and 292 eV)
6	76.2 eV	40.21 eV	4th resonance of U238 (66 eV)
7	40.21 eV	22.6 eV	3rd resonance of U238 (36.7 eV)
8	22.6 eV	19.08 eV	2nd resonance of U238 (20.9 eV)
9	19.08 eV	7.6 eV	Resonances of even isotopes
10	7.6 eV	4.0 eV	1st resonance of U238
11	4.0 eV	0.625 eV	1st resonance of Pu240 and Pu242
12	0.625 eV	0.9 eV	1st resonance of U235, Pu239 and Pu241
13	0.9 eV	0.1 meV	Thermal domain

In the present study, we perform comparisons on regular UOX and MOX cell lattices for different void fractions in order to mainly pinpoint errors due to self-shielding only (other multigroup issues such scattering anisotropy treatment are not very important in this case, which is not true in more heterogeneous patterns).

The different self-shielding methods of APOLLO3® are recalled in Chapter 2 and numerical results in Chapter 3.

2. APOLLO3® SELF-SHIELDING MODELS

In APOLLO3®, the three models, Sanchez-Coste, Subgroup and Tone, are based on the integral form of the transport equation discretized by the collision probability method CP (although the two latter can also apply on the integro-differential form):

$$V_j \Sigma_{t,j}(u)\phi_j(u) = \sum_i V_i P_{ij}(u) Q_i(u) \qquad (1)$$

2.1 Sanchez-Coste method

2.1.1. Separate treatment of the resonant isotopes

In the original Livolant-Jeanpierre formalism, the resonant isotopes are treated separately and the source $Q_i(u)$ in Eq. (1) is assumed to be a pure elastic scattering source, so that this equation is transformed into a slowing-down equation:

$$\left(\Sigma_{t,j}^{*}(u) + \Sigma_{t,j}^{+}(u)\right) V_j \phi_j(u) = \sum_i P_{ij}(u) V_i \left(R_i^{*}\left(\phi_i(u)\right) + R_i^{+}\left(\phi_i(u)\right)\right) \qquad (2)$$

where we separated the resonant nuclide (*) from the "moderator" nuclides (+).

The slowing down process is supposed to be elastic and isotropic in the center of mass. The slowing down operators can be written:

$$R_i^{*} = N_i^{*} r^{*} \qquad\qquad R_i^{+} = \sum_{l \neq *} N_i^{l} r^{l}$$

with the usual expression (for example for the resonant isotope):

$$r^{*}\left(\phi(u)\right) = \int_{u-\varepsilon^{*}}^{u} \frac{e^{(u'-u)}}{1-\alpha^{*}} \sigma_s^{*}(u') \phi(u') du' \qquad (3)$$

The Livolant-Jeanpierre formalism makes the fundamental assumption that the maximal lethargy gain on the "moderator" is much larger than on the resonant isotope one ($\varepsilon^{+} \gg \varepsilon^{*}$)[3] so that the strong flux variations due to the resonances are smoothed and, thus, the macroscopic flux $\Psi_i(u)$ defined by:

$$\Psi_i(u) = \frac{R_i^{+}\left(\phi(u)\right)}{\Sigma_{s,i}^{+}(u)}$$

varies slowly with the lethargy. In addition, this function is assumed spatially uniform in the Sanchez-Coste model: $\Psi_i(u) = \Psi(u)$. The flux $\phi_i(u)$ is then factorized into the product of this macroscopic flux and a fine structure function $\varphi_i(u)$:

$$\phi_i = \varphi_i \Psi$$

$\Psi(u)$ is assumed constant between lethargies u and $u - \varepsilon^{*}$, i.e:

$$R_i^{*}(\phi_i) = R_i^{*}(\varphi_i \Psi) \approx \Psi R_i^{*}(\varphi_i)$$

Replacing ϕ_i by $\varphi_i \Psi$ in the slowing-down equation leads to the *fine structure equation*:

[3] This assumption is no more valid when light nuclei are removed (in case of voiding for the fuel) or for media containing nuclei of intermediate mass (such as metallic bulks).

$$\varphi_j(u) = \sum_i \frac{V_i P_{ij}(u)}{V_j \Sigma_{t,j}(u)} \left(\Sigma_{s,i}^{+}(u) + N_i^* \, r^*\left(\varphi_i(u)\right) \right) \tag{4}$$

Within the statistical hypothesis, the heavy slowing-down operator can be replaced by the average of the scattering reaction rate over group g:

$$r^*\left(\varphi_i(u)\right) \approx \langle \sigma_s^* \varphi_i^{ST} \rangle_g = \tau_{s,i}^{ST,g} \qquad \text{if} \;\; u_{g-1} \le u \le u_g$$

Reporting this approximation in (4), multiplying by σ_s^* and summing over group g leads to a system of coupled source equations whose unknowns are the microscopic scattering rates of the resonant isotope in the different regions:

$$\tau_{s,j}^{ST,g} = \sum_i \frac{V_i}{V_j} \langle \frac{\sigma_s^* P_{ij}}{\Sigma_{t,j}} \rangle_g \left(\Sigma_{s,i}^{+,g} + N_i^* \, \tau_{s,i}^{ST,g} \right) \tag{5}$$

The diffusion cross sections of the non-resonant isotopes have been supposed constant on group g:

$$\Sigma_{s,i}^{+}(u) = \Sigma_{s,i}^{+,g} \qquad\qquad u_{g-1} \le u \le u_g$$

The integrals $\langle \frac{\sigma_s^* P_{ij}}{\Sigma_{t,j}} \rangle_g$ in Eq. (5) are independent of the flux and calculated using CALENDF-type probability tables $\left(\omega^k, \sigma_t^k, \sigma_s^k, \sigma_{a,}^k, \sigma_f^k\right)_{k \in [1,K]}$ [10, 11] obtained on the 281-group energy mesh:

$$\langle \frac{\sigma_\rho^* P_{ij}}{\Sigma_{t,j}} \rangle_g = \sum_{k=1}^{K} \omega^k \frac{\sigma_\rho^k P_{ij}^k}{N_i^* \sigma_t^k + \Sigma_{t,i}^{+,g}} \tag{6}$$

where P_{ij}^k is calculated for each base point σ_t^k.

Once system (5) is solved, the fine structure in the statistical model is obtained from Eq. (4)

$$\varphi_j^{ST} = \sum_i \frac{V_i P_{ij}}{V_j \Sigma_{t,j}} \left(\Sigma_{s,i}^{+,g} + N_i^* \, \tau_{s,i}^{ST,g} \right)$$

and the "effective" reaction rate can be calculated for any reaction ρ

$$\tau_{\rho,j}^{ST,g} = \langle \sigma_\rho^* \varphi_j^{ST} \rangle_g = \sum_i \frac{V_i}{V_j} \langle \frac{\sigma_\rho^* P_{ij}}{\Sigma_{t,j}} \rangle_g \left(\Sigma_{s,i,g}^{+} + N_i^* \, \tau_{s,i}^{ST,g} \right) \tag{7}$$

still using the probability tables to get the integrals $\langle \frac{\sigma_\rho^* P_{ij}}{\Sigma_{t,j}} \rangle_g$.

For an infinite homogeneous medium, the fine structure equation is reduced to Eq. (8)

$$(\sigma_t^*(u)+\sigma_b)\varphi(u) = r^*\big(\varphi(u)\big)+\gamma_b\sigma_b \qquad (8)$$

with the dilution cross section $\sigma_{b=}\frac{\Sigma_{t,hom}^{+,g}}{N^*}$ and the ratio $\gamma_b=\frac{\Sigma_{s,hom}^{+,g}}{\Sigma_{t,hom}^{+,g}}$ taking into account the "moderator" absorption.

Within the statistical assumption, the fine structure is obtained directly:

$$\varphi^{ST}(u) = \frac{1}{1-\langle\frac{\sigma_s^*}{\sigma_t^*+\sigma_b}\rangle_g}\frac{\gamma_b\sigma_b}{\sigma_t^*(u)+\sigma_b}$$

and so, for the reaction rates

$$\tau_{\rho,hom}^{ST,g} = \frac{\gamma_b\sigma_b}{1-\langle\frac{\sigma_s^*}{\sigma_t^*+\sigma_b}\rangle_g}\langle\frac{\sigma_\rho^*}{\sigma_t^*+\sigma_b}\rangle_g$$

The heterogeneous-homogeneous equivalence consists for each heterogeneous region j and group g in finding the corresponding dilution cross section for the homogeneous medium that gives the same absorption rates, i.e. finding σ_b such that the following equality is verified (non-linear problem):

$$\tau_{a,hom}^{ST,g}(\sigma_b) = \tau_{a,j}^{ST,g}$$

When the value of σ_b is obtained, it is used to interpolate the "exact" homogeneous absorption rates in pre-calculated tables (the fine structure equation has been solved previously for each resonant isotope with the exact scattering operator and an ultrafine energy mesh for different values of σ_b and the temperature). It is assumed that if there is equality between the heterogeneous and homogeneous rates under the statistical hypothesis, this equality remains for the exact slowing-down, i.e.:

$$\tau_{\rho,hom}^{ST,g}(\sigma_b) = \tau_{\rho,j}^{ST,g} \;\Rightarrow\; \tau_{\rho,j}^{*,\mathrm{g}} = \tau_{\rho,hom}^{*,g}(\sigma_b)$$

Once obtained the reference reaction rates $\tau_{\rho,j}^{*,g}$, a SPH equivalence is performed to get the self-shielded total cross section $\sigma_{t,j}^{*,\mathrm{g}}$ allowing the conservation of the total reaction rates in the multigroup problem:

$$\sigma_{t,j}^{*,\mathrm{g}}\varphi_j^g = \tau_{t,j}^{*,g}$$

with the flux φ_j^g solution of a coarse energy mesh fine structure equation (also a non-linear problem):

$$\varphi_j^g = \sum_i \frac{P_{ij}\big(\Sigma_t^g\big)V_i}{\left(N_j^*\sigma_{t,j}^{*,g}+\Sigma_{t,j}^{+,g}\right)V_j}\left(\Sigma_{s,i}^{+,g}+N_i^*\sum_{g'\le g}p_\infty^{*,g'\to g}\tau_{s,i}^{*,g}\right) \qquad (9)$$

$p_{\infty}^{*,g'\to g}$ is the non-self-shielded multigroup transfer probability.

2.1.2. Treatment of a resonant mixture

Coste and Mengelle extended the Livolant-Jeanpierre model to a mixture of resonant isotopes m [18] to account for mutual shielding. Without giving the details, the procedure globally follow the same principles than with one single isotope:

- a fine structure equation is derived for the mixture considered as a single isotope with total cross section
$$\sigma_t^*(u) = \frac{\sum_m N_m^* \sigma_{t,m}^*(u)}{\sum_m N_m^*}$$
- the 281-group probability tables of the mixture depending of the relative abundances $\frac{N_m^*}{\sum_m N_m^*}$, they are calculated on the fly using fine probability tables (more than 11000 groups) provided by CALENDF for the different isotopes. Each partial reaction of each resonant isotope is considered as a partial reaction of the mixture:
$$\left(\omega^k, \sigma_t^k, \sigma_{s,m}^k, \sigma_{a,m}^k, \sigma_{f,m}^k\right)_{k\in[1,K],\ m\in[1,M]}$$
- the TR slowing-down model (more precise than the ST statistical one) is used to get the fine structure and the reactions rates for the different isotopes and reaction of the mixture
- dilution cross sections are obtained for each resonant isotope
- given the dilution cross sections, the fine structure equation in infinite homogeneous media is solved on the fly for each isotope to get the "exact" reference reaction rates (pre-tabulation is not possible because the relative abundances are not known in advance),
- the SPH equivalence is performed to get finally the self-shielded cross sections.

In the APOLLO2 calculation schemes currently recommended by CEA [19], this mixture self-shielding treatment is used for the significant isotopes of Uranium and Plutonium in the range [33 eV ; 200 eV], the ST model being used on the outside separately for each isotope.

2.2. Subgroup method of ECCO

The fundamental assumption in the subgroup method of ECCO is the absence of correlation between the sources and the reactions at lethargy u so that, after energy integration, Eq. (1) leads to:

$$\langle \phi_j \rangle_g = \sum_i \frac{V_i}{V_j} \langle \frac{P_{ij}}{\Sigma_{t,j}} Q_i \rangle_g \approx \sum_i \frac{V_i}{V_j} \langle \frac{P_{ij}}{\Sigma_{t,j}} \rangle_g \langle Q_i \rangle_g \tag{10}$$

and

$$\langle \sigma_\rho^* \phi_j \rangle_g = \sum_i \frac{V_i}{V_j} \langle \sigma_\rho^* \frac{P_{ij}}{\Sigma_{t,j}} Q_i \rangle_g \approx \sum_i \frac{V_i}{V_j} \langle \sigma_\rho^* \frac{P_{ij}}{\Sigma_{t,j}} \rangle_g \langle Q_i \rangle_g \tag{11}$$

$\langle\frac{P_{ij}}{\Sigma_{t,j}}\rangle_g$ and $\langle\sigma_\rho^*\frac{P_{ij}}{\Sigma_{t,j}}\rangle_g$ are calculated using the CALENDF-type probability tables as in the Sanchez-Coste method. The multigroup sources $\langle Q_i\rangle_g$ are updated during the power iterations.

At convergence, the self-shielded cross sections are given by the ratio:

$$\sigma_{\rho,j}^{*,g} = \frac{\langle\sigma_\rho^*\phi_j\rangle_g}{\langle\phi_j\rangle_g} = \frac{\sum_{k=1}^{K}\frac{\sum_i V_i\omega^k\sigma_\rho^k\,P_{ij}^k\,Q_i^g}{\left(N_j^*\sigma_t^k+\Sigma_{t,j}^{+,g}\right)}}{\sum_{k=1}^{K}\frac{\sum_i V_i\omega^k\,P_{ij}^k\,Q_i^g}{\left(N_j^*\sigma_t^k+\Sigma_{t,j}^{+,g}\right)}} \qquad (12)$$

The 383-energy structure possesses 142 energy groups between 22.6 eV and 11.14 keV. Such a number makes it possible to satisfy the non-correlation hypothesis, to avoid a specific mutual shielding treatment and the superhomogenization (SPH) procedure.

2.3. Tone's Method

For the sake of simplicity, our presentation of the Tone method differs from its real implementation in APOLLO3® [7].

In the Tone method, the source (fission + slowing-down) is assumed constant in each group g ($Q_i(u)\approx Q_i^g$) but its fundamental assumption is that the flux $\phi_{ij}(u)$ in region j due to neutrons emitted in region i is proportional to the multigroup flux ϕ_{ij}^g with a coefficient $\alpha_j(u)$ depending only on the arrival region j:

$$\phi_{ij}(u) = \frac{V_i}{V_j}\frac{P_{ij}(u)}{\Sigma_{tj}(u)}Q_i(u) \approx \frac{V_i}{V_j}\frac{P_{ij}(u)}{\Sigma_{tj}(u)}Q_i^g \approx \alpha_j(u)\frac{V_i}{V_j}\frac{P_{ij}^g}{\Sigma_{tj}^g}Q_i^g = \alpha_j(u)\phi_{ij}^g$$

Using the reciprocity and conservation relations:

$$V_i\Sigma_{ti}(u)P_{ij}(u) = V_j\Sigma_{tj}(u)P_{ji}(u) \qquad \sum_i P_{ji}(u) = 1$$

the flux $\phi_j(u)=\sum_i\phi_{ij}(u)$ can be written as:

$$\phi_j(u) = \frac{\sum_i V_i\,P_{ij}^g Q_i^g}{\sum_i V_i(N_i^*\,\sigma_t^*(u)+\Sigma_{t,i}^{+,g})P_{ij}^g}\ , \qquad u\in g$$

with the following expression for $\alpha_j(u)$:

$$\alpha_j(u) = \frac{V_j\Sigma_{tj}^g}{\sum_i V_i(N_i^*\,\sigma_t^*(u)+\Sigma_{t,i}^{+,g})P_{ij}^g}\ , \qquad u\in g$$

The self-shielded cross-sections are obtained using the probability tables again:

$$\sigma_{\rho,j}^{*,g} = \frac{\langle \sigma_\rho^* \phi_j \rangle_g}{\langle \phi_j \rangle_g} = \frac{\left\langle \frac{\sigma_\rho^*}{\sum_i V_i (N_i^* \sigma_t^*(u) + \Sigma_{t,i}^{+,g}) P_{ij}^g} \right\rangle_g}{\left\langle \frac{1}{\sum_i V_i (N_i^* \sigma_t^*(u) + \Sigma_{t,i}^{+,g}) P_{ij}^g} \right\rangle_g} = \frac{\sum_{k=1}^K \frac{\omega^k \sigma_\rho^k}{\sum_i V_i (N_i^* \sigma_t^k + \Sigma_{t,i}^{+,g}) P_{ij}^g}}{\sum_{k=1}^K \frac{\omega^k}{\sum_i V_i (N_i^* \sigma_t^k + \Sigma_{t,i}^{+,g}) P_{ij}^g}}$$

but only the CPs by group needs to be calculated in comparison with the subgroup or the Sanchez-Coste methods where the CPs must be calculated for each base point k of the probability tables (cf. Eq. (6) and (12)). Furthermore, the cross-sections are independent of the source value and can be obtained before the flux calculation (as for the Sanchez-Coste method).

3. NUMERICAL RESULTS

Figure 1 depicts the spatial mesh used to calculate infinite lattices of UOX and MOX fuel pins. This mesh allows taking into account the increasing thermal flux going to each corner of the elementary cell and the collapsing of the flux entering the fuel at energies of resonances; the pellet is split in four concentric regions to perform spatial distributed self-shielding calculations (50 %, 30 %, 15 % and 5 % of the volume). Several temperature conditions have been analyzed: isothermal configurations at 20°C (CZP) and 300°C (HZP), a "full power" configuration with a temperature of 300°C in water and clad and a uniform temperature of 600°C in fuel (HFP) and a last configuration with a given temperature gradient in the pellet: 500°C, 700°C, 900°C and 1100°C (GRADT). Two partial voided (40% and 80%) and a full voided (100%) situation have also be analyzed for the MOX.

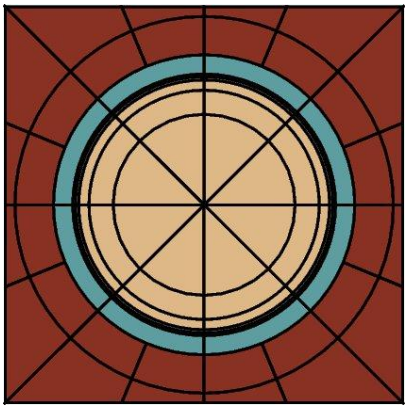


Figure 1. UOX and MOX Cell spatial mesh.

The tracking parameters of the Method of Characteristics have been optimized (48 angles $\in [0, \pi]$ for the uniform azimuthal quadrature, 3 angles $\in [0, \pi/2]$ for the Bickley polar quadrature, uniform track density of 100 cm^{-1}). The scattering anisotropy is P3.

For the UOX and MOX cells, the comparison of the three methods with respect to TRIPOLI-4® are reported in Table II and IV respectively for the multiplication factor and the integrated absorption rates of the main heavy isotopes. A detailed analysis of ^{238}U absorption over the 4 rings and 13 energy groups of Table I is presented Table III for the UOX at HFP conditions and Table V to Table XIII for the MOX HFP with different void fractions and for the temperature gradient in the fuel Table IX. The reaction rates are normalized to a total production of 100 000 neutrons; the absolute differences are thus expressed in pcm. No self-shielding model is applied below 22.6 eV (group 8 and more).

Table II. UOX and MOX: APOLLO3/TRIPOLI-4 comparisons on multiplication factors and main integrated absorption rates.

		Sanchez-Coste SHEM281	Subgroup REL383	Tone REL383
UOX iso 20°C	k_{inf} (pcm)	-15	-22	-116
	^{238}U (pcm)	30	44	145
	^{235}U (pcm)	20	16	-71
UOX iso 300°C	k_{inf} (pcm)	-101	-82	-185
	^{238}U (pcm)	59	54	155
	^{235}U (pcm)	-47	-31	-121
UOX fuel 600°C	k_{inf} (pcm)	-121	-97	-199
	^{238}U (pcm)	78	72	167
	^{235}U (pcm)	-65	-49	-133
UOX Temp Gradient	k_{inf} (pcm)	-40	-42	510
	^{238}U (pcm)	1	27	-514
	^{235}U (pcm)	-6	-7	-471

Table III. UOX fuel 600°C: AP3-T4 comparisons on detailed ^{238}U absorption rates (pcm).

	Sanchez-Coste SHEM281					Subgroup REL383					Tone REL383				
ring	1	2	3	4	Tot	1	2	3	4	Tot	1	2	3	4	Tot
g1	-4	-3	-1	0	-9	-3	-3	-1	0	-7	-3	-3	-1	0	-7
g2	-2	-2	-1	0	-5	-2	-2	-1	0	-4	-2	-2	-1	0	-4
g3	-7	-4	-2	-1	-13	1	0	0	0	1	1	0	0	0	1
g4	5	4	3	0	13	9	6	2	1	18	59	8	-12	-8	47
g5	3	5	12	15	34	-10	-5	-5	-6	-26	184	16	-69	-64	67
g6	-10	-9	-1	10	-10	8	6	1	-2	12	12	13	-1	-12	12
g7	22	2	-12	21	33	11	12	13	1	37	16	33	14	-30	35
g8	3	5	12	3	23	4	5	12	3	24	2	4	11	2	20
g9	0	0	0	0	1	0	0	0	0	1	0	0	0	0	0
g10	8	8	6	0	22	9	8	6	0	23	7	6	5	-1	16
g11	0	0	0	0	0	0	0	0	0	0	-1	0	0	0	-1
g12	2	1	0	0	3	2	1	0	0	3	1	1	0	0	2
g13	-7	-4	-2	-1	-14	-7	-4	-2	-1	-14	-9	-6	-3	-1	-20
Tot	15	2	15	47	78	21	25	26	-4	68	268	70	-57	-113	167

Table IV. MOX: AP3-T4 comparisons on multiplication factors and main integrated absorption rates.

		Sanchez-Coste	Subgroup	Tone
MOX iso 20°C	k_{inf} (pcm)	-76	-75	-186
	^{238}U (pcm)	22	6	134
	^{239}Pu (pcm)	-10	7	-96
	^{240}Pu (pcm)	13	34	4
	^{241}Pu (pcm)	-4	-12	-20
	^{242}Pu (pcm)	16	12	9
MOX iso 300°c	k_{inf} (pcm)	-152	-128	-247
	^{238}U (pcm)	66	16	119
	^{239}Pu (pcm)	-60	-19	-82
	^{240}Pu (pcm)	-7	26	9
	^{241}Pu (pcm)	-4	-10	-21
	^{242}Pu (pcm)	16	12	8
MOX fuel 600°C	k_{inf} (pcm)	-213	-157	-275
	^{238}U (pcm)	107	30	134
	^{239}Pu (pcm)	-93	-34	-96
	^{240}Pu (pcm)	-13	23	4
	^{241}Pu (pcm)	-6	-9	-20
	^{242}Pu (pcm)	15	12	9
MOX Temp Gradient	k_{inf} (pcm)	-103	-176	505
	^{238}U (pcm)	10	42	-487
	^{239}Pu (pcm)	-35	-41	269
	^{240}Pu (pcm)	9	26	105
	^{241}Pu (pcm)	4	-11	58
	^{242}Pu (pcm)	20	13	29
MOX 40% void	k_{inf} (pcm)	-280	-229	-274
	^{238}U (pcm)	155	-23	135
	^{239}Pu (pcm)	-116	-61	-80
	^{240}Pu (pcm)	-57	-19	-24
	^{241}Pu (pcm)	0	-6	-11
	^{242}Pu (pcm)	16	9	8
MOX 80% void	k_{inf} (pcm)	-388	-201	-101
	^{238}U (pcm)	235	-144	81
	^{239}Pu (pcm)	-146	-43	-4
	^{240}Pu (pcm)	-141	-84	-69
	^{241}Pu (pcm)	-1	7	15
	^{242}Pu (pcm)	7	-5	-2
MOX 100% void	k_{inf} (pcm)	714	-9	-14
	^{238}U (pcm)	-536	-3	-3
	^{239}Pu (pcm)	216	-12	-14
	^{240}Pu (pcm)	54	7	6
	^{241}Pu (pcm)	53	1	1
	^{242}Pu (pcm)	12	2	2

Table V. MOX Void 0%: AP3-T4 comparisons on detailed ^{238}U absorption rates (pcm).

	Sanchez-Coste 281g					Subgroup 383g					Tone 383g				
ring	1	2	3	4	Tot	1	2	3	4	Tot	1	2	3	4	Tot
g1	-4	-5	-2	-1	-12	-3	-4	-2	0	-10	-3	-4	-2	0	-10
g2	-1	-2	-1	0	-5	-1	-2	-1	0	-4	-1	-2	-1	0	-4
g3	-14	-7	-4	-1	-25	1	0	0	0	2	1	0	0	0	2
g4	9	9	6	2	26	10	6	3	1	19	60	8	-12	-8	48
g5	4	20	27	15	67	-22	-12	-8	-7	-49	167	9	-71	-64	41
g6	-6	-8	7	8	1	12	8	2	-2	21	15	15	1	-10	20
g7	12	1	6	16	35	5	9	11	1	26	10	28	13	-28	23
g8	3	4	11	3	21	4	5	11	3	23	3	4	11	2	19
g9	-1	-1	0	0	-2	-1	-1	0	0	-2	-1	-1	0	0	-2
g10	4	5	4	-2	11	5	5	4	-1	13	3	4	3	-3	7
g11	-1	-1	0	0	-2	-1	0	0	0	-2	-1	-1	0	0	-2
g12	-1	0	0	0	-1	0	0	0	0	-1	-1	0	0	0	-1
g13	-3	-2	-1	0	-7	-3	-2	-1	0	-6	-3	-2	-1	0	-7
Tot	2	13	52	39	107	5	12	19	-6	30	248	58	-61	-112	134

Table VI. MOX Void 40%: AP3-T4 comparisons on detailed ^{238}U absorption rates (pcm).

	Sanchez-Coste 281g					Subgroup 383g					Tone 383g				
ring	1	2	3	4	Tot	1	2	3	4	Tot	1	2	3	4	Tot
g1	-7	-6	-2	-1	-15	-3	-3	-1	0	-7	-3	-3	-1	0	-7
g2	-2	-2	-1	0	-5	-1	-2	-1	0	-4	-1	-2	-1	0	-4
g3	-26	-14	-7	-2	-50	1	1	0	0	2	2	1	0	0	3
g4	19	18	10	4	50	16	11	4	1	33	85	13	-16	-11	72
g5	17	37	42	22	117	-46	-24	-17	-11	-98	203	5	-97	-84	28
g6	-3	-9	9	11	8	14	10	3	-2	25	19	18	1	-13	25
g7	19	2	6	21	47	3	7	11	0	20	10	31	12	-34	18
g8	2	3	11	2	17	3	4	11	2	20	2	3	11	2	18
g9	-2	-1	-1	0	-4	-2	-1	-1	0	-4	-2	-1	-1	0	-4
g10	0	2	2	-4	0	1	2	2	-3	1	0	1	2	-4	-1
g11	-2	-1	-1	0	-4	-2	-1	-1	0	-4	-2	-1	-1	0	-4
g12	-1	-1	0	0	-2	-1	-1	0	0	-2	-1	-1	0	0	-2
g13	-2	-2	-1	0	-5	-2	-2	-1	0	-5	-2	-2	-1	0	-6
Tot	12	25	66	51	155	-19	1	10	-15	-23	310	62	-91	-146	135

Table VII. MOX Void 80%: AP3-T4 comparisons on detailed ^{238}U absorption rates (pcm).

	Sanchez-Coste 281g					Subgroup 383g					Tone 383g				
ring	1	2	3	4	Tot	1	2	3	4	Tot	1	2	3	4	Tot
g1	-11	-7	-3	-1	-22	-4	-3	-1	0	-7	-4	-3	-1	0	-7
g2	1	0	0	0	1	2	0	0	0	3	2	0	0	0	3
g3	-91	-52	-26	-8	-178	2	1	0	0	2	4	2	0	0	6
g4	70	54	26	8	159	36	26	8	1	72	141	27	-22	-17	129
g5	77	83	69	33	261	-99	-50	-32	-18	-199	208	-20	-132	-107	-50
g6	10	-4	8	11	25	15	10	3	-2	27	21	18	2	-13	29
g7	34	6	1	18	60	-4	2	6	-2	2	7	23	7	-31	5
g8	-8	-4	4	-2	-10	-2	0	6	0	4	-1	1	7	0	7
g9	-6	-4	-2	-1	-12	-5	-3	-1	0	-10	-5	-3	-1	0	-9
g10	-15	-9	-6	-7	-38	-11	-6	-3	-5	-26	-10	-5	-2	-5	-22
g11	-4	-3	-1	0	-8	-4	-2	-1	0	-7	-3	-2	-1	0	-6
g12	-1	-1	0	0	-2	-1	0	0	0	-1	-1	0	0	0	-1
g13	-1	-1	0	0	-2	-1	-1	0	0	-2	-1	-1	0	0	-2
Tot	55	60	70	51	235	-76	-26	-15	-27	-144	360	38	-144	-173	81

Table VIII. MOX Void 100%: AP3-T4 comparisons on detailed ^{238}U absorption rates (pcm).

	Sanchez-Coste 281g					Subgroup 383g					Tone 383g				
ring	1	2	3	4	Tot	1	2	3	4	Tot	1	2	3	4	Tot
g1	-17	-10	-4	-1	-32	-15	-9	-3	-1	-29	-15	-9	-3	-1	-29
g2	43	26	13	4	85	38	23	12	4	76	38	23	12	4	76
g3	-467	-274	-138	-46	-925	-18	-13	-9	-4	-44	-17	-14	-10	-4	-44
g4	132	92	45	15	284	2	3	-3	-2	0	25	-2	-14	-8	1
g5	20	16	10	4	50	-4	-1	-1	0	-7	3	-2	-5	-3	-7
Tot	-288	-150	-74	-24	-536	3	3	-5	-4	-3	34	-4	-20	-13	-3

Table IX. MOX with temperature gradient: AP3-T4 comp. on detailed ^{238}U absorption rates (pcm).

	Sanchez-Coste 281g					Subgroup 383g					Tone 383g				
ring	1	2	3	4	Tot	1	2	3	4	Tot	1	2	3	4	Tot
g1	2	-1	0	0	1	-3	-4	-2	0	-10	-3	-4	-2	0	-10
g2	-6	-5	-2	-1	-13	-1	-2	-1	0	-4	-1	-2	-1	0	-4
g3	-10	-7	-3	-1	-22	-1	-1	-1	0	-3	-5	-3	-2	-1	-11
g4	1	6	5	-1	11	13	10	1	-1	23	-54	-41	-27	-11	-133
g5	-57	-4	24	16	-21	-31	-7	-3	-9	-50	-126	-118	-100	-65	-409
g6	-14	-21	-3	12	-27	11	10	3	-3	21	-19	-10	-12	-10	-51
g7	34	9	-18	15	39	9	8	5	2	23	13	9	-3	-13	6
g8	11	1	8	5	26	14	3	9	5	31	22	9	14	10	54
g9	-1	0	0	0	-1	-1	-1	0	0	-2	1	1	0	0	3
g10	19	4	2	0	25	18	3	1	-1	21	31	13	10	8	62
g11	-1	0	0	0	-1	-1	-1	0	0	-2	1	1	0	0	3
g12	-1	0	0	0	-1	-1	0	0	0	-1	0	0	0	0	1
g13	-2	-2	-1	0	-5	-3	-2	-1	0	-6	0	0	0	0	0
Tot	-25	-20	9	45	10	24	15	10	-8	42	-139	-145	-121	-82	-487

The best agreements with TRIPOLI-4®, both in space and energy, are obtained for all situations with the subgroup method and the 383-group energy mesh:

- the error on the multiplication factor is less than 100 pcm for UOX (Table II), 160 pcm for MOX in the non-voided case and reach a maximum of -230 pcm in the 40%-void case (Table IV),
- only small compensations are observed between the absorption rates of the heavy isotopes,
- the spatial and energetic distribution of ^{238}U is well reproduced with a maximum error of 200 pcm for the 80%-void case in group 5 (energy range 76 eV -750 eV) where the resonances are not finely described (Table VII),
- in the presence of a temperature gradient (Table IX), results are also satisfactory.

For UOX and MOX non-voided cases, the Sanchez-Coste results are a little less accurate than the subgroup ones; the slight overestimation of the ^{238}U absorption in the external ring r4, both in UOX and MOX, represent only 0.3% of the total absorption of that isotope. Larger discrepancies appears for the MOX when voiding: the error on multiplication factor start from -180 pcm for the HFP non-voided configuration, increases up to -500 pcm for the 80%-void configuration to become almost 0 in the 100%-void one. The void effect is then poorly calculated by mean of this method (the Tone's method performs better for this parameter).

For a uniform fuel temperature, the results with the Tone's method of APOLLO3® are surprisingly good, regarding those obtained by Hébert with DRAGON5. They are a little bit less accurate than the subgroup ones with an underestimation of the infinite multiplication factor of 200 pcm in UOX and 275 pcm in MOX for the non-voided configuration. ^{238}U absorption is overestimated in the resolved resonance energy range where self-shielding models are applied (between 10 keV and 22.6 eV, corresponding to groups 4 to 7): by 160 pcm for UOX and 130 pcm for MOX (about 0.5 % of the total absorption). The spatial distribution shows a small drift: absorption rates are overestimated by 250 pcm in the center and underestimated by 110 pcm in the external ring (respectively 2.4% and 3.7 % of the total ^{238}U absorption of the ring, which is about four times lower than the discrepancies reported in [16]). Unlike the other two methods, the discrepancies on multiplication factor against TRIPOLI-4® are reducing with the void fraction (despites a small increase of the drift of the spatial distribution for the 40% and 80%-void cases). However, the case with a temperature gradient is poorly calculated. The ^{238}U absorption rates are no longer overestimated but underestimated by 500 pcm.

In the different cases, the Tone results are very close to the subgroup ones in the first three groups (20 MeV - 11 keV). The comparison over the 383-group energy mesh (Figure 2) shows that this consistency continues down to about 3 keV (group 75). The Tone's method can thus replace the subgroup method above this limit without loss of precision. The gain in CPU time will be estimated in the final paper from more representative 2D assembly calculations; at the cell level, the number of calculated Pij is divided by two.

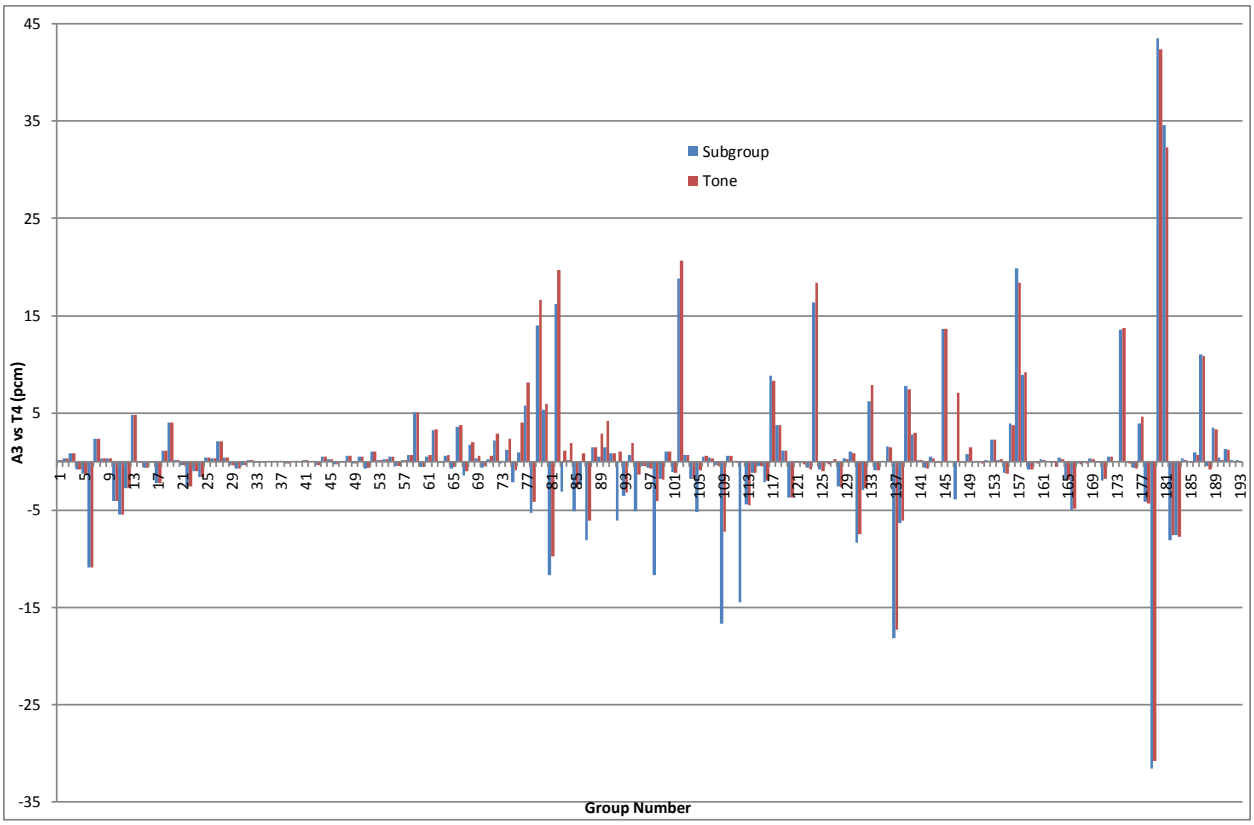


Figure 2. MOX cell Void 0%: APOLLO3 Tone and subgroup comparisons with TRIPOLI-4® on 383-group ^{238}U absorption rates (pcm)

4. CONCLUSIONS

The numerical validation of the three self-shielding methods of APOLLO3® on UOX and MOX infinite lattice calculations shows the following results:

- the ECCO subgroup method using the REL383 energy mesh provide accurate results in all kind of situations and can be considered as a reference self-shielding method for Light Water Reactor,
- the legacy Sanchez-Coste method, based on a heterogeneous-homogeneous equivalence, is almost as performant for non-voided configurations but is less accurate in case of voiding,
- the Tone's method overestimates a little the ^{238}U capture under 3 keV but the errors remain limited in most of the situations, specifically in case of voiding. Only the configurations with a fuel temperature gradient are poorly calculated.
- the Tone's method can be substituted at the subgroup method for E > 3 keV without loss of precision, allowing a significant reduction of the calculation time (by a factor of 2). It can be used alone for less demanding design studies (in terms of accuracy), provided a uniform temperature distribution in fuel.

ACKNOWLEDGMENTS

APOLLO3® and TRIPOLI-4® are registered trademark of CEA. We gratefully acknowledge CEA, AREVA and EDF for their long-term partnership and their support. We would like to thank also the APOLLO3® development team for their efforts in implementing the models described here.

REFERENCES

1. D. Schneider, F. Dolci, F. Gabriel, J. Palau, M. Guillo and B. Pothet, "APOLLO3®: CEA/DEN Deterministic Multi-purpose code for Reactor Physics Analysis," *Proc. Int. Conf. on Physics of Reactors, PHYSOR2016*, Sun Valley, Idaho, USA, May 1–5, 2016.
2. R. Sanchez, I. Zmijarevic, M. Coste-Delclaux, M. Masiello, S. Santandrea, E. Martinolli, L. Villate, N. Schwartz et N. Guler, "APOLLO2 year 2010," *Nuclear Engineering and Technology*, vol. 42, pp. 474-499, 2010.
3. G. Rimpault, "Algorithmic features of the ECCO cell code for treating heterogeneous fast reactor assemblies," *Proc. Int. Conf. on Mathematics and Computation, M&C95*, Portland, Oregon, USA, April 30-May 4, 1995
4. D. Sciannandrone, S. Santandrea, R. Sanchez and L. Li Mao, "Coupled fine-group three dimensional flux calculation and subgroups method for a FBR hexagonal assembly with the APOLLO3® core physics analysis code," in *Proc. Int. Conf. on Mathematics and Computation, M&C2015*, April 19–23, 2015
5. P. Archier, J.-M. Palau, J.-F. Vidal, V. R. G. Pascal and B. Roque, "New Reference APOLLO3 Calculation Sheme for Sodium Cooled Fast reactors: from Sub-Assembly tu Full-Core Calculations," *Proc. Int. Conf. on Physics of Reactors, PHYSOR2016*, Sun Valley, Idaho, USA, May 1–5, 2016
6. T. Tone, "A Numerical Study of Heterogeneity Effects in Fast Reactor Critical Assemblies," *Nuclear Science and Technology*, vol. 12, n° 8, pp. 467-481, 1975
7. L. Li Mao, I. Zmijarevic and R. Sanchez, "Resonance Self-Shielding Methods for Fast Reactor Calculations—Comparison of a New Tone's Method with the Subgroup Method in APOLLO3®," *Nuclear Science and Engineering*, vol. 188, n° 1, pp. 15-32, 2017
8. M. Livolant et F. Jeanpierre, *Autoprotection des résonances dans les réacteurs nucléaires, Rapport CEA - R-4533*, 1974
9. A. Canbakan, A. Hébert and J.-F. Vidal, "Validation of a Subgroup Method for Pressurized Water Reactor Fuel Assembly Model," *Proc. Int. Conf. on Mathematics and Computation, M&C2015*, Nashville, Tennessee, USA, April 19-23, 2015.
10. P. Ribon and J.-M. Maillard, "Les tables de probabilité : Application au traitement des sections efficaces pour la neutronique," Note CEA-N-2485, 1986
11. J.-Ch. Sublet, P. Ribon and M. Coste-Delclaux: "CALENDF-2010 : User Manual Rapport," Rapport CEA-R-6277, ISSN 0429-3460, 2011
12. J.-F. Vidal, R. Le Tellier, P. Blaise, G. Guillot, N. Huot, O. Litaize, A. Santamarina, N. Thiollay and C. Vaglio-Gaudard, "Analysis of the FLUOLE experiment for the APOLLO2 validation of PWR core reflectors," in *Proc. Int. Conf on the Physics of Reactors, PHYSOR2008*, Interlaken, Switzerland, September 14-19, 2008
13. N. Hfaiedh and A. Santamarina, "Determination of the Optimized SHEM Mesh for Neutron Transport Calculations," *Proc. Int. Conf. on Mathematics and Computation, M&C2005*, Avignon, France, September 12-15, (2005)

14. A. Hébert and A. Santamarina, "Refinement of the Santamarina-Hfaiedh Energy Mesh Between 22.5 eV and 11.4 keV," *Proc. Int. Conf. PHYSOR 2008*, Interlaken, Switzerland, September 14–19, (2008)
15. A. Hébert, "Application of Tone's and embedded self-shielding method to pressurized reactor assemblies", *Annals of Nuclear Energy*, **112**, pp.439-449 (2018).
16. A. Hébert, "An investigation of distributed self-shielding effects with the Tone's method", *Proc. Int. Conf. on the Physics of Reactors, PHYSOR 2018*, Cancun, Mexico, (2018)
17. E. Brun et al., "TRIPOLI-4®, CEA, EDF and AREVA reference Monte Carlo code," Annals of Nuclear Energy, **vol. 82**, pp. 151-160, 2015.
18. M. Coste-Delclaux and S. Mengelle, "New resonant mixture self-shielding treatment in the code APOLLO2," in *Proc. Int. Conf. on the Physics of Reactors, PHYSOR 2004*, Chicago, Illinois, USA, 2004
19. A. Santamarina, D. Bernard, P. Blaise, P. Leconte, J-M. Palau, B. Roque, C. Vaglio, J-F. Vidal, "Validation of the new code package APOLLO2.8 for accurate PWR neutronics calculations," *Int. Conf. on Mathematics and Computation, M&C 2013*, Sun Valley, USA, May 5-9, 2013.
20. www.polymlt.ca/merlin/librairies.htm